Ab Initio MO Study of the CO_2 Insertion into the Cu(I)−R Bond (R = H, CH_3, or OH). Comparison between the CO_2 Insertion and the C_2H_4 Insertion

Shigeyoshi Sakaki* and Yasuo Musashi

Department of Applied Chemistry, Faculty of Engineering, Kumamoto University, Kurokami, Kumamoto 860 Japan

Received November 24, 1993[⊗]

Ab initio MO/MP4, SD−CI, and CCD (coupled cluster (doubles)) calculations are carried out on the insertion reactions of CO_2 and C_2H_4 into the Cu−R (R = H, CH_3, and OH) bond. The insertion into the Cu−CH_3 bond occurs with a higher activation energy than the corresponding insertion into the Cu−H bond. This is because $Cu(CH_3)(PH_3)_2$ distorts at the TS to a greater extent than $CuH(PH_3)_2$, due to the highly directional sp^3 valence orbital of CH_3 unlike the spherical 1s valence orbital of H. The CO_2 insertion into the Cu−H and Cu−CH_3 bonds occurs with a lower activation energy and a higher exothermicity than the C_2H_4 insertion. The higher exothermicity of the CO_2 insertion is because the Cu−OC(O)R bond is stronger than the Cu−CH_2CH_2R bond. The reason for the lower activation energy is that the π orbital of CO_2 lies at lower energy level than that of C_2H_4; accordingly, the exchange repulsion between R and CO_2 is smaller than that between R and C_2H_4. The CO_2 insertion into the Cu−OH bond proceeds with no barrier. The main reason is that the lone-pair orbital of OH, which is not used for coordination to Cu, can form a bonding interaction between OH and CO_2 without weakening of the Cu−OH bond.

Introduction

CO_2 insertion into the M−R (R = H, CH_3, or OR) bond has received considerable interest in the chemistry of CO_2 fixation[1] because similar insertion reactions of alkene, alkyne, and CO are involved as key processes in many homogeneous catalytic cycles.[2] Actually, many examples of the catalytic CO_2 conversion into organic chemicals involve the CO_2 insertion as an important elementary step.[3−12] General knowledge about the CO_2 insertion is, therefore, necessary to a good understanding of the CO_2 fixation and finding a new efficient catalyst for the CO_2 fixation. In this context, experimental investigation of the CO_2 insertion has been actively carried out, in which various valid data have been reported.[13−32] Not only experimental work but also theoretical work is expected to offer such general

[⊗] Abstract published in *Advance ACS Abstracts,* March 1, 1995.

(1) For instance; (a) Darensbourg, D. J.; Kudaroski, R. A. *Adv. Organomet. Chem.* **1983**, *22*, 129. (b) Palmer, D. A.; van Eldik, R. *Chem. Rev.* **1983**, *83*, 651. (c) Walther, D. *Coord. Chem. Rev.* **1987**, *79*, 135. (d) Behr, A. *Angew. Chem., Int. Ed. Engl.* **1988**, *27*, 661. (e) Braustein, P.; Matt, D.; Nobel, D. *Chem. Rev.* **1988**, *88*, 747. (f) Culter, A. R.; Hanna, P. K.; Vites, J. C. *Chem. Rev.* **1988**, *88*, 1363. (g) Behr, A. *Carbon Dioxide Activation by Metal Complexes*; VCH Publishing: Weinheim, Germany, 1988.

(2) For instance; (a) Alexander, J. J. In *The Chemistry of the Metal-Carbon Bond*; Hartley, F. R.; Patai, S., Ed.; John Wiley & Sons: New York, 1985; Vol. 2, p 339. (b) *The Chemistry Metal-Carbon Bond*; Hartley, F. R.; Patai, S., Ed.; John Wiley & Sons: New York, 1985; Vol. 3. (c) Crabtree, R. H. *The Organometallic Chemistry of Transition Metals*, John Wiley & Sons, New York, 1988.

(3) (a) Inoue, S.; Takeda, N. *Bull. Chem. Soc. Jpn.* **1977**, *50*, 984. (b) Aida, T.; Inoue, S. *J. Am. Chem. Soc.* **1983**, *105*, 1304. (c) Kojima, F.; Aida, T.; Inoue, S. *J. Am. Chem. Soc.* **1986**, *108*, 391. (d) Aida, T.; Ishikawa, M.; Inoue, S. *Macromolecules* **1986**, *19*, 8. (e) Hirai, Y.; Aida, T.; Inoue, S. *J. Am. Chem. Soc.* **1989**, *111*, 3062. (f) Komatsu, M.; Aida, T.; Inoue, S. *J. Am. Chem. Soc.* **1991**, *113*, 8492.

(4) Rokicki, A.; Kuran, W. *J. Macromol. Sci. Rev. Macromol. Chem.* **1981**, *135*, C21.

(5) Soga, K.; Imai, E.; Hattori, I. *Polym. J.* **1981**, *13*, 407.

(6) Gambarotta, S.; Strologo, S.; Floriani, C.; Chiesi-Villa, A.; Guastini, C. *J. Am. Chem. Soc.* **1985**, *107*, 6278.

(7) (a) Carmona, E.; Palma, P.; Paneque, M.; Poveta, M. L. *J. Am. Chem. Soc.* **1986**, *108*, 6424. (b) Carmona, E.; Gutiérrez-Puebla, E.; Marin, J. M.; Monge, A.; Paneque, M.; Poveta, M. L.; Ruiz, C. *J. Am. Chem. Soc.* **1989**, *111*, 2883.

(8) Braunstein, P.; Matt, D.; Nobel, D. *J. Am. Chem. Soc.* **1988**, *110*, 3207.

(9) Darensbourg, D. J.; Ovalles, C. *J. Am. Chem. Soc.* **1989**, *109*, 3330.

(10) Aye, K. T.; Gelmini, L.; Payne, N. C.; Vittal, J. J.; Puddephatt, R. J. *J. Am. Chem. Soc.* **1990**, *112*, 2464.

(11) (a) Amatore, C.; Jutand, A. *J. Am. Chem. Soc.* **1991**, *113*, 2819. (b) Amatore, C.; Jutand, A. *J. Electroanal. Chem.* **1991**, *306*, 141.

(12) Tsai, J. C.; Nicholas, K. M. *J. Am. Chem. Soc.* **1992**, *114*, 5117.

(13) (a) Pu, L. S.; Yamamoto, A.; Ikeda, S. *J. Am. Chem. Soc.* **1968**, *90*, 3896. (b) Komiya, S.; Yamamoto, A. *J. Organomet. Chem.* **1972**, *46*, C58. (c) Miyashita, A.; Yamamoto, A. *J. Organomet. Chem.* **1973**, *49*, C57. (d) Ikariya, T.; Yamamoto, A. *J. Organomet. Chem.* **1974**, *72*, 145. (e) Miyashita, A.; Yamamoto, A. *J. Organomet. Chem.* **1976**, *113*, 187. (f) Komiya, S.; Yamamoto, A. *Bull. Chem. Soc. Jpn.* **1976**, *49*, 784. (g) Yamamoto, T.; Kubota, M.; Yamamoto, A. *Bull. Chem. Soc. Jpn.* **1980**, *53*, 680.

(14) Misono, A.; Uchida, Y.; Hidai, M.; Kuse, T. *J. Chem. Soc., Chem. Commun.* **1968**, 981.

(15) Zucchini, V.; Albizzati, E.; Giannini, V. *J. Organomet. Chem.* **1971**, *26*, 357.

(16) (a) Tsuda, T.; Saegusa, T. *Inorg. Chem.* **1972**, *11*, 2561. (b) Tsuda, T.; Ueda, T. *J. Chem. Soc., Chem. Commun.* **1974**, 380. (c) Tsuda, T.; Chujo, Y.; Saegusa, T. *J. Chem. Soc., Chem. Commun.* **1975**, 963. (d) Tsuda, T.; Sanada, S.; Ueda, K.; Saegusa, T. *Inorg. Chem.* **1976**, *15*, 2329. (e) Tsuda, T.; Chujo, Y.; Saegusa, T. *J. Am. Chem. Soc.* **1978**, *100*, 630. (f) Tsuda, T.; Chujo, Y.; Saegusa, T. *J. Am. Chem. Soc.* **1980**, *102*, 431.

(17) Kolomnikov, I. S.; Gusev, A. I.; Aleksandrov, G. G.; Lobeeva, T. S.; Struchkov, Yu. I.; Vol'pin, M. E. *J. Organomet. Chem.* **1973**, *59*, 349.

(18) Cahiez, G.; Normant, J. F.; Bernard, D. *J. Organomet. Chem.* **1975**, *94*, 463.

(19) Karsch, H. H. *Chem. Ber.* **1977**, *110*, 2213.

(20) Koinuma, H.; Yoshida, Y.; Hirai, H. *Chem. Lett.* **1975**, 1223.

(21) Inoue, Y.; Izumida, H.; Sasaki, Y.; Hashimoto, H. *Chem. Lett.* **1976**, 863.

(22) (a) Chisholm, M. H.; Reichert, W. W.; Cotton, F. A.; Murillo, C. A. *J. Am. Chem. Soc.* **1977**, *99*, 1652. (b) Chisholm, M. H.; Cotton, F. A.; Extine, M. W.; Reichert, W. W. *J. Am. Chem. Soc.* **1978**, *100*, 1727.

(23) Yoshida, T.; Thorn, D. L.; Okano, T.; Ibers, J. A.; Ohtsuka, S. *J. Am. Chem. Soc.* **1979**, *101*, 4212.

(24) Van Eldik, R.; Palmer, D. A.; Kelm, H.; Harris, G. M. *Inorg. Chem.* **1980**, *19*, 3679.

(25) Razuvaef, G. A.; Vyshinskaya, L. I.; Drobotenko, V. V.; Malkova, G. Y.: Vysinski, N. N. *J. Organomet. Chem.* **1982**, *239*, 335.

(26) Marsich, N.; Camus, N.; Nardin, G. *J. Organomet. Chem.* **1982**, *239*, 429.

0020-1669/95/1334-1914$09.00/0

knowledge. However, only few MO studies have been carried out on the CO_2 insertion.[33,34] In those studies, the geometry of transition state (TS) has not been optimized, and calculation at the correlated level has not been performed except for preliminary MP2 calculations of the CO_2 insertion into the Cu(I)−H and Cu(I)−CH_3 bonds.[33]

In this work, the CO_2 insertion into the Cu(I)−R bond (R = H, CH_3, or OH) is theoretically investigated with the ab initio MO/MP4, SD-CI, and CCD (coupled cluster (doubles)) methods.

$$CuR(PH_3)_2 + CO_2 \rightarrow Cu(\eta^1\text{-}OCOR)(PH_3)_2 \rightarrow Cu(\eta^2\text{-}O_2CR)(PH_3)_2 \quad (1)$$

This reaction is selected here, considering that there are many experimental reports on the insertion reactions of CO_2 into Cu(I)−alkyl,[13c−e,16b,e,18,26,27q] Cu(I)−hydride,[28] and Cu(I)−alkoxide bonds.[13g,16a,d,f] Our aims in this work are (a) to optimize the geometry of the TS, (b) to estimate the activation energy and the energy of reaction, (c) to reveal characteristic features of the CO_2 insertion by comparing it with the C_2H_4 insertion (eq 2), and (d) to clarify the factors determing the ease of the CO_2

$$CuR(PH_3)_2 + C_2H_4 \rightarrow Cu(CH_2CH_2R)(PH_3)_2 \quad (2)$$

insertion. Points of departure from previous works[33,34] are presenting (i) detailed knowledge of the TS structure and (ii) discussion based on the calculations at the correlated level.

Computational Details

Ab initio closed-shell Hartree−Fock (HF), MP2−MP4(SDQ), SD−CI, and coupled cluster (doubles; CCD) calculations were carried out with Gaussian 86[35a] and 92[35b] programs, where four kinds of basis sets were employed. In the small basis set (BS I), core electrons of Cu (up to 3p) were replaced with effective core potentials (ECP1) given by Hay et al.[36] and its 3d, 4s, and 4p valence orbitals were represented with a (3s 2p 5d)/ [2s 2p 2d] set. The usual MIDI-3[37] and (4s)/[2s][38] sets were used for C, O, and H respectively. STO-2G[39] sets were employed for PH_3. In the second (BS II), core electrons of Cu (up to 2p) were replaced with effective core potentials (ECP2), and its valence orbitals (3s, 3p, 3d, 4s, and 4p) were represented with a (5s 5p 5d)/[3s 3p 3d] set.[40] The usual MIDI-4 sets[37] were used for C, O, and P, and the (4s)/[2s] set was employed for H.[38] In the third (BS III), an all electron type basis set was used for Cu; Huzinaga's (13s 7p 4d) primitive set[37] was augmented with one diffuse d primitive function (ζ = 0.141)[41] and two p primitive functions describing the valence 4p orbital, and the resultant (13s 9p 5d) primitive set was contracted to a [5s 4p 3d] set. For the other atoms, the same basis sets as those in BS II were used. In the fourth (BS IV), (9s 5p)/[3s 2p][38] sets were used for C and O. For Cu, a (14s 9p 5d) primitive set of Wachters[42] was augmented with one diffuse d primitive function (ζ = 0.1491) given by Hay[43] and two p primitive functions (ζ = 0.155 065 and 0.046 199) describing the valence 4p orbitals.[44] The resultant (14s 11p 6d) primitive set was contracted to a [5s 4p 3d] set. For PH_3, the same basis sets as those in the BS II and BS III were used. The BS I set was used only for geometry optimization, the BS II−IV sets were used for examination of basis set effects, and the BS III set was used for discussion of energy change, electron redistribution, and change in bonding nature by the insertion reactions. Calculations at the correlated level were performed with all the core orbitals excluded from an active space.

Both insertion reactions of CO_2 and C_2H_4 are considered to proceed via the precursor complexes (PC) and TS, as shown in Scheme 1. Geometries of CO_2, C_2H_4, $CuR(PH_3)_2$ (**1**) (see Scheme 1 for **1**−**10**), PC (**2**, **7**), TS (**3**, **8**), and products (**4**−**6**, **9**, **10**) were optimized with the energy gradient method at the HF level, in which the geometry of PH_3 was fixed to the experimental structure of the free PH_3 molecule.[45] There are several possible isomers in the products; see **4**−**6** in the CO_2 insertion and **9** and **10** in the C_2H_4 insertion. **4A** and **4B** could not be optimized since they converted to **5A** and **5B**, respectively, with no barrier.[33] Their MO calculations were carried out, assuming the geometry of the OC(O)R group and the Cu−O distance to be the same as those in **5A** and **5B**. Because **5B** converted to **6B** with no barrier, the geometry of **5B** was optimized on the assumption that the Cu−O^1 bond was fixed on the $Cu(PH_3)_2$ plane. Geometries of **9A** and **9B** were optimized under the constraint of C_s symmetry. In the CO_2 insertion into the Cu−OH bond, PC and TS could not be optimized because this reaction proceeded with no barrier at both HF and correlated levels (vide infra). Geometry changes by this insertion were optimized, taking the distance between O of OH and C of CO_2 as a reaction coordinate.

Results and Discussion

Effects of Basis Set and Electron Correlation on the CO_2 and C_2H_4 Insertions. Prior to detailed discussion, we will

(27) (a) Darensbourg, D. J.; Rokicki, A. *J. Am. Chem. Soc.* **1982**, *104*, 349. (b) Slater, S. G.; Lusk, R.; Schumann, B. F.; Darensbourg, M. *Organometallics*, **1982**, *1*, 1662. (c) Darensbourg, D. J.; Rokicki, A. *Organometallics* **1982**, *1*, 1685. (d) Darensbourg, D. J.; Pala, M.; Waller, J. *Organometallics*. **1983**, *2*, 1285. (e) Darensbourg, D. J.; Kudaroski, R. *J. Am. Chem. Soc.* **1984**, *106*, 3672. (f) Darensbourg, D. J.; Ovalless, C. *J. Am. Chem. Soc.* **1984**, *106*, 3750. (g) Darensbourg, D. J.; Pala, M. *J. Am. Chem. Soc.* **1984**, *107*, 5687. (h) Darensbourg, D. J.; Hanckel, R. K.; Bauch, C. G.; Pala, M.; Simmons, D.; White, J. N. *J. Am. Chem. Soc.* **1985**, *107*, 7463. (i) Darensbourg, D. J.; Grötsch, G. *J. Am. Chem. Soc.* **1985**, *107*, 7473. (j) Darensbourg, D. J.; Bauch, C. G.; Rheingold, A. L. *Inorg. Chem.* **1987**, *26*, 977. (k) Darensbourg, D. J.; Sanchez, K. M.; Rheingold, A. L. *J. Am. Chem. Soc.* **1987**, *109*, 290. (l) Darensbourg, D. J.; Grötsch, G.; Wiegreffe, P.; Rheingold, A. L. *Inorg. Chem.* **1987**, *26*, 3827. (m) Darensbourg, D. J.; Darensbourg, M. Y.; Goh, L. Y.; Ludvig, M.; Wiegreffe, P. *J. Am. Chem. Soc.* **1987**, *109*, 7539. (n) Darensbourg, D. J.; Sanchez, K. M.; Reibenspies, J. H.; Rheingold, A. L. *J. Am. Chem. Soc.* **1989**, *111*, 7094. (o) Darensbourg, D. J.; Wiegreffe, H. P.; Riordan, C. G. *J. Am. Chem. Soc.* **1990**, *112*, 5759. (p) Darensbourg, D. J.; Wiegreffe, H. P.; Wiegreffe, P. W. *J. Am. Chem. Soc.* **1990**, *112*, 9252. (q) Darensbourg, D. J.; Mueller, B. L.; Bischoff, C. J.; Chojnacki, S. S. *Inorg. Chem.* **1991**, *30*, 2418.

(28) Bianchini, C.; Ghilardi, C. A.; Meli, A.; Midollini, S.; Orlandini, A. *Inorg. Chem.* **1985**, *24*, 924.

(29) Cocolios, P.; Guilard, R.; Bayeul, D.; Lecomte, C. *Inorg. Chem.* **1985**, *24*, 2058.

(30) Kaska, W. C.; Nemeh, S.; Shirazi, A.; Potuznik, S. *Organometallics* **1988**, *7*, 13.

(31) Arai, T.; Sato, Y.; Inoue, S. *Chem. Lett.* **1990**, 551.

(32) Hartwig, J. F.; Bergman, R. G.; Andersen, R. A. *J. Am. Chem. Soc.* **1991**, *113*, 6499.

(33) (a) Sakaki, S.; Ohkubo, K. *Inorg. Chem.* **1988**, *27*, 2020. (b) Sakaki, S.; Ohkubo, K. *Inorg. Chem.* **1989**, *28*, 2583. (c) Sakaki, S.; Ohkubo, K. *Organometallics* **1989**, *8*, 2970.

(34) Bo, C.; Dedieu, A. *Inorg. Chem.* **1989**, *28*, 304.

(35) (a) Frisch, M. J.; Binkley, J. S.; Schlegel, H. B.; Raghavachari, K.; Melius, C. F.; Martin, R. L.; Stewart, J. J. P.; Bobrowicz, F. W.; Rohlfing, C. M.; Kahn, L. R.; DeFrees, D. J.; Seeger, R.; Whiteside, R. A.; Fox, D. J.; Fluder, E. M.; Topiol, S.; Pople, J. A. *Gaussian 86*; Carnegie-Mellon Quantum Chemistry Publishing Unit; Pittsburgh, PA, 1986. (b) Frisch, M. J.; Trucks, G. W.; Head-Gordon, M.; Gill, P. M. W.; Wong, M. W.; Foresman, J. B.; Johnson, B. G.; Schlegel, H. B.; Robb, M. A.; Replogle, E. S.; Gomperts, R.; Andres, J. L.; Raghavachari, K.; Binkley, J. S.; Gonzalez, C.; Martin, R. L.; Fox, D. J.; DeFrees, D. J.; Baker, J.; Stewart, J. J. P.; Pople, J. A. *Gaussian 92*; Gaussian, Inc.: Pittsburgh PA, 1992.

(36) Hay, P. J.; Wadt, W. R. *J. Chem. Phys.* **1985**, *82*, 270.

(37) Huzinaga, S.; Andzelm, J.; Klobukowski, M.; Radzio-Andzelm, E.; Sakai, Y.; Tatewaki, H. *Gaussian Basis Sets for Molecular Calculations*; Elsevier: Amsterdam, 1984.

(38) Dunning, T. H.; Hay, P. J. In *Methods of Electronic Structure Theory*; Schaefer, H. F., Ed.; Plenum: New York, 1977; p 1.

(39) Hehre, W. J.; Stewart, R. F.; Pople, J. A. *J. Chem. Phys.* **1969**, *51*, 2657.

(40) Hay, P. J.; Wadt, W. R. *J. Chem. Phys.* **1985**, *82*, 299.

(41) This exponent was determined, according to an even-tempered criterion.

(42) Wachters, A. J. H. *J. Chem. Phys.* **1970**, *52*, 1033.

(43) Hay, P. J. *J. Chem. Phys.* **1977**, *66*, 4377.

(44) Original exponents which mainly represent 4p orbitals of Cu were used not directly but after scaling up by a factor 1.5, to make them suitable for molecular calculation.[42]

(45) Herzberg, G. *Molecular Spectra and Molecular Structure*; D. Van Nostrand Co. Inc.: Princeton, NJ, 1967; Vol. 3, p 610.

Scheme 1

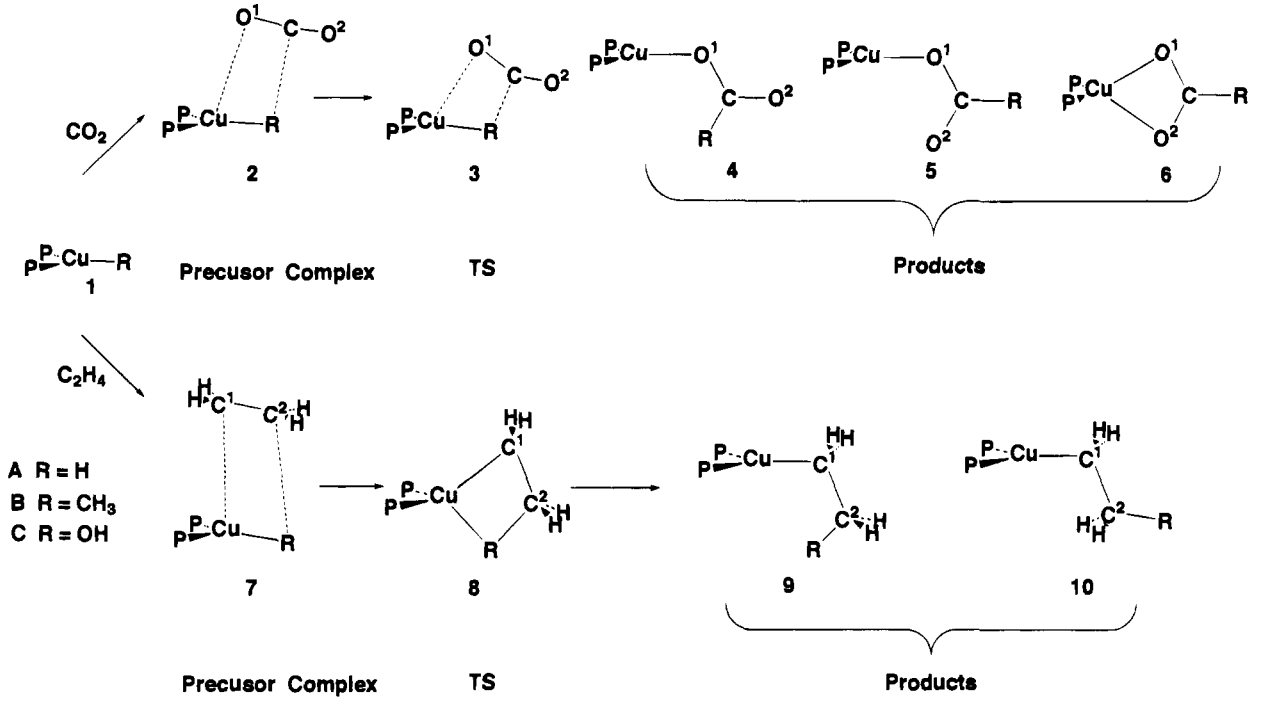

Table 1. Effects of Basis Sets and Electron Correlation for CO_2 and C_2H_4 Insertions into the Cu−H bond (kcal/mol)

(A) Basis Set Effects at the Hartree−Fock Level (CO_2 Insertion into the Cu−H Bond)

	BS I	BS II	BS III	BS IV	BS V[a]	BS VI[b]
E_a[c]	7.0	3.7	4.2	1.6	12.5	5.4
ΔE[d]	−38.9	−50.4	−48.5	−53.8	−37.5	−56.8

(B) Electron correlation effects

	HF	MP2	MP3	MP4(DQ)	MP4(SDQ)	SD−CI	SD−CI + D[e]	SD−CI + DS[f]	SD−CI + P[g]
					(a) CO_2 Insertion into the Cu−H Bond				
E_a	4.2	8.3	2.2	6.5	7.9	4.5	5.3	4.2	4.3
ΔE	−48.5	−30.1	−43.9	−36.0	−33.1	−43.1	−41.0	−40.0	−39.7
					(b) C_2H_4 Insertion into the Cu−H Bond				
E_a	23.3	2.7	11.6	6.8	2.0	6.8	2.0	12.6	9.9
ΔE	−13.5	−19.4	−16.5	−15.2	−18.3	−16.9	−16.8	−16.3	−16.4

[a] BS V (BS II of ref 33b). The basis set for Cu was the same as it in BS I, while the basis sets for the other part were the same as those in BS IV. [b] BS VI (BS III of ref 33b). The basis sets for Cu, C, and O were the same as those in BS III, while MIDI-3 was used for PH_3. [c] E_a = the energy difference between the transition state and the precursor complex (PC). [d] ΔE = the energy difference between product and PC. [e] D = the Davidson correction for higher order excitations.[47] [f] DS = the Davidson and Silver correction for higher order excitations.[48] [g] P = the Pople correction for higher order excitations.[49]

briefly examine basis set effects on the CO_2 insertion into the Cu-H bond. As shown in Table 1A, the activation energy, E_a, and the energy difference between the PC and the product, ΔE, significantly decrease upon going to BS V from BS VI,[33b] whereas only the basis set for Cu is different between BS V and BS VI; in BS VI, a (3s 2p 5d)/[2s 2p 2d] set is employed with the ECP1,[36] but in BS VI, an all electron type basis set[42] is used (see footnotes *a* and *b* of Table 1 for BS V and BS VI). Similarly, E_a and ΔE considerably decrease upon going to BS II from BS I. On the other hand, BS II, BS III, and BS IV yield similar values for E_a and ΔE. These results lead to the following findings: (1) E_a and ΔE do not depend much on the basis sets of ligand atoms but significantly depend on the ECPs for Cu, (2) Huzinaga's basis set and Wachters' one for Cu give similar results for E_a and ΔE, (3) the basis set involving the ECP1 yields considerably different results from others, and (4) BS II involving ECP2 yields almost the same results as the better basis sets such as BS III and BS IV. Thus, use of either BS II or better basis sets is necessary in estimating the energy change. Very recently, use of ECP2 has also been recommended.[46]

Then, we will inspect the correlation effects on E_a and ΔE (Table 1B). Unexpectedly, E_a of the CO_2 insertion little changes upon introducing electron correlation, except that the E_a value slightly fluctuates at the MP2 level. On the other hand, introduction of electron correlation considerably changes the E_a of the C_2H_4 insertion and the ΔE of both CO_2 and C_2H_4 insertion reactions. An important result to be noted is that both E_a of the C_2H_4 insertion and ΔE of CO_2 and C_2H_4 insertion reactions considerably fluctuate at MP2−MP4(SDQ) levels, demonstrating that the MP2−MP4(SDQ) methods are not reliable in investigating these insertion reactions. On the other hand, SD−CI and CCD methods give similar results on E_a and ΔE, suggesting that these methods are reliable (see Tables 1B, 2, and 3). The discussion presented below is based on the SD−CI and CCD calculations with BS-III.

(46) (a) Hay, P. J. *New. J. Chem.* **1991**, *15*, 735. (b) Leininger, T.; Riehl, J.-F.; Jeung, G.-H.; Pélissier, M. *Chem. Phys. Lett.* **1993**, *205*, 301.
(47) Langhoff, S. R.; Davidson, E. R. *Int. J. Quantum Chem.* **1974**, *8*, 61.
(48) Davidson, E. R.; Silver, D. W. *Chem. Phys. Lett.* **1977**, *52*, 403.
(49) Pople, J. A.; Seeger, R.; Krishnan, R. *Int. J. Quantum Chem. Symp.* **1977**, *11*, 149.

Table 2. Energy Change by CO_2 Insertion into the Cu−R (R = H, CH_3) Bond (kcal/mol)

		MP4(SDQ)	SDCI−DS[a]	CCD
(A) CO_2 Insertion into the Cu−H Bond				
$CuH(PH_3)_2$ (**1A**) + CO_2		0.0[b]	0.0[c]	0.0[d]
precursor complex	**2A**	−4.5	−5.0	−4.7
transition state	**3A**	3.4	−0.8	−0.4
Cu(η^1-OCOH)$(PH_3)_2$	**4A**	−22.3	−28.4	
	5A	−35.2	−42.1	
Cu(η^2-O_2CH)$(PH_3)_2$	**6A**	−37.0	−44.5	−44.7
(B) CO_2 Insertion into the Cu−CH_3 Bond				
Cu(CH_3)$(PH_3)_2$ (**1B**) + CO_2		0.0[e]	0.0[f]	
precursor complex	**2B**	−5.2	−5.2	
transition state	**3B**	10.5	4.1	
Cu(η^1-OCOCH_3)$(PH_3)_2$	**4B**	−13.2	−20.6	
	5B	−39.0	−47.1	
Cu(η^2-O_2CCH_3)$(PH_3)_2$	**6B**	−40.7	−49.1	

[a] DS = Davidson−Silver's correction for higher order excitations.[48] [b] E_t(MP4(SDQ)) = −2510.0628 [c] E_t(SDCI + (DS)) = −2510.0080 [d] E_t = −2509.9929 [e] E_t(MP4(SDQ)) = −2549.1425 [f] E_t(SDCI + (DS)) = −2549.0848 (hartree units).

Table 3. Energy Change by C_2H_4 Insertion into the Cu−R (R = H, CH_3) Bond (kcal/mol)

compd		MP4(SDQ)	SDCI−DS[a]	CCD
(A) C_2H_4 insertion into the Cu−H bond				
$CuH(PH_3)_2$ (**1A**) + C_2H_4		0.0[b]	0.0[c]	0.0[d]
precursor complex	**7A**	−1.2	1.3	−0.8
transition state	**8A**	0.8	6.7	9.7
Cu(C_2H_5)$(PH_3)_2$	**9A**	−16.4	−14.5	
	10A	−19.5	−17.6	−16.4
(B) C_2H_4 Insertion into the Cu−CH_3 Bond				
Cu(CH_3)$(PH_3)_2$ **1B** + C_2H_4		0.0[e]	0.0[f]	
precursor complex	**7B**	−2.8	1.0	
transition state	**8B**	22.5	23.4	
Cu(C_3H_7)$(PH_3)_2$	**9B**	−11.5	−11.2	
	10B	−18.9	−18.3	

[a] DS = Davidson−Silver correction for higher order excitations.[48] [b] E_t(MP4(SDQ)) = −2400.5232 [c] E_t(SDCI + (DS)) = −2400.4794 [d] E_t(CCD) = −2400.4669 [e] E_t(MP4(SDQ)) = −2439.6029 [f] E_t(SDCI + (DS)) = −2439.5565 (hartree units).

Relative Stabilities of the Products and the Energy of Reaction. Relative stabilities of the products are given in Tables 2 and 3 as an energy difference from the sum of reactants, **1A** + CO_2, **1A** + C_2H_4, **1B** + CO_2, and **1B** + C_2H_4, where a negative value represents a stabilization energy (and vice versa).

In the product of the CO_2 insertion, **6A** and **6B** are calculated to be the most stable in **4A**−**6A** and **4B**−**6B**, respectively, suggesting that Cu(η^2-O_2CR)$(PH_3)_2$ is a final product of the CO_2 insertion.[33] Relative stabilities of these products have been discussed in our previous work[33b] and the discussion is omitted here. Both CO_2 insertion reactions into the Cu−H and Cu−CH_3 bonds are significantly exothermic, and the exothermicity of the former is slightly greater than that of the latter.

In the product of the C_2H_4 insertion, **10A** and **10B** are calculated to be more stable than **9A** and **9B**, respectively, indicating that **10A** and **10B** are final products. The exothermicity of the C_2H_4 insertion reaction hardly depends on the kind of R.

One of the differences between CO_2 insertion and C_2H_4 insertion is that the former is much more exothermic than the latter. This difference is rationalized in terms of bond energies.[50] In the CO_2 insertion into the Cu−CH_3 bond, the CH_3−C(O)O− bond is newly formed, and the Cu−CH_3 and =C=O bonds change to the Cu−OC(O)CH_3 and =C(O−)− bonds respectively. Thus, the exothermicity (E_{exo}) is approximately represented by eq 3. In the C_2H_4 insertion into the Cu−CH_3 bond,

$$E_{exo} = E(\text{Cu}-\text{OC(O)CH}_3) + E(=\text{C(O}-)-) + E(\text{CH}_3-\text{C(O)O}-) - E(\text{Cu}-\text{CH}_3) - E(=\text{C=O})$$

$$E_{exo} = \{E(\text{Cu}-\text{OC(O)CH}_3) - E(\text{Cu}-\text{CH}_3)\} + \{E(=\text{C(O}-)-) - E(=\text{C=O})\} + E(\text{CH}_3-\text{C(O)O}-) \quad (3)$$

the Cu−CH_3 and >C=C< bonds change to the Cu−C_3H_7 and the −CH_2−CH_2− bond respectively, and the −CH_2−CH_3 bond is newly formed. In this case, E_{exo} is approximately represented, as follows:

$$E_{exo} = E(\text{Cu}-\text{C}_3\text{H}_7) - E(\text{Cu}-\text{CH}_3) + E(-\text{CH}_2-\text{CH}_3) + E(-\text{CH}_2-\text{CH}_2-) - E(\text{C=C}) \sim \{E(-\text{CH}_2-\text{CH}_2-) - E(>\text{C=C}<)\} + E(-\text{CH}_2-\text{CH}_3) \quad (4)$$

E(Cu−CH_3) is considered to be almost the same as E(Cu−C_3H_7).

A difference between =C=O and =C(O−)− bond energies appearing in eq 3 can be estimated from the energy difference (ΔE_{r-1}) between right- and left-hand sides of eq 5, as follows:

$$\text{CO}_2 + \text{H}_2 \rightarrow \text{H}-\text{C(O)OH} \quad (5)$$

$$\Delta E_{r-1} = E(\text{H}-\text{H}) + E(=\text{C=O}) - E(=\text{C(O}-)-) - E(=\text{C(H)}-) - E(-\text{O}-\text{H}) \quad (6a)$$

$$E(=\text{C=O}) - E(=\text{C(O}-)-) = \Delta E_{r-1} - E(\text{H}-\text{H}) + E(=\text{C(H)}-) + E(-\text{O}-\text{H}) \quad (6b)$$

Similarly, a difference between the >C=C< and −CH_2−CH_2− bond energies can be estimated from ΔE_{r-1} of eq 7:

$$\text{C}_2\text{H}_4 + \text{H}_2 \rightarrow \text{H}_3\text{C}-\text{CH}_3 \quad (7)$$

$$\Delta E_{r-1} = E(\text{H}-\text{H}) + E(>\text{C=C}<) - E(\gtrdot\text{C}-\text{C}\lessdot) - 2E(\gtrdot\text{C}-\text{H}) \quad (8a)$$

$$E(>\text{C=C}<) - E(\gtrdot\text{C}-\text{C}\lessdot) = \Delta E_{r-1} - E(\text{H}-\text{H}) + 2E(\gtrdot\text{C}-\text{H}) \quad (8b)$$

In these estimations, the H−H and ⩾C−H bond energies are calculated with MP2−MP4(SDQ) and SD−CI/BS III methods (Table 4), where geometries of $^{\bullet}C_2H_5$, $^{\bullet}$C(O)OH, and H−C(O)−O$^{\bullet}$ radicals are optimized with the ROHF/BS I method. A difference between Cu−CH_3 and Cu−OC(O)R bond energies can be evaluated, considering the energy difference between right- and left-hand sides of eq 9, where −O−H and H−C(O)−

$$\text{Cu}(\text{CH}_3)(\text{PH}_3)_2 + \text{H}-\text{OC(O)R} \rightarrow \text{Cu}(\text{OC(O)R})(\text{PH}_3)_2 + \text{H}-\text{CH}_3 \quad (9)$$

$$\Delta E_{r-1} = E(\text{H}-\text{CH}_3) + E(\text{Cu}-\text{OC(O)R}) - E(\text{Cu}-\text{CH}_3) - E(-\text{O}-\text{H}) \quad (10a)$$

$$E(\text{Cu}-\text{OC(O)R}) - E(\text{Cu}-\text{CH}_3) = \Delta E_{r-1} - E(\text{H}-\text{CH}_3) - E(-\text{O}-\text{H}) \quad (10b)$$

OR bond energies can be estimated as described above. Using these bond energies and their differences (Table 4), a difference in E_{exo} between CO_2 and C_2H_4 insertion reactions can be easily

(50) We discuss the exothermicity of Cu(η^1-OC(O)R)$(PH_3)_2$ (**5A**, **5B**, or **5C**) here, because the final product, Cu(η^2-O_2CR)$(PH_3)_2$ (**6A**, **6B**, or **6C**) is only slightly more stable than **5A**, **5B**, and **5C**, respectively (see Table 2 and Figure 5).

Table 4. Bond Energies and Their Differences (kcal/mol)

	E(H–H)	E(H–COOH)	E(HCOO–H)	E(H–CH_3)	E(H$_3$C–CH_3)	E(H–C_2H_5)	E(C=O) – E(C–O)	E(C=C) – E(C–C)	E(H$_3$C–COOH)	E(HO–COOH)	E(HOCOO–H)	E(HO–H)	E(Cu–OC(O)CH$_3$) – E(Cu–CH$_3$)	E(Cu–OC(O)H) – E(Cu–H)	E(Cu-OCOOH) – E(Cu–OH)
MP4(SDQ)	97.5	98.0	103.7	100.5	58.7	102.3	106.5	72.0	92.0	87.1	100.7	100.8	49.4	37.5	29.5
SD–CI + DS[a]	97.9	93.8	102.1	100.4	58.1	104.4	102.6	74.6	86.7	64.3	99.5	98.7	55.6	34.4	29.5

[a] DS = Davidson-Silver's correction for higher order excitations.[48]

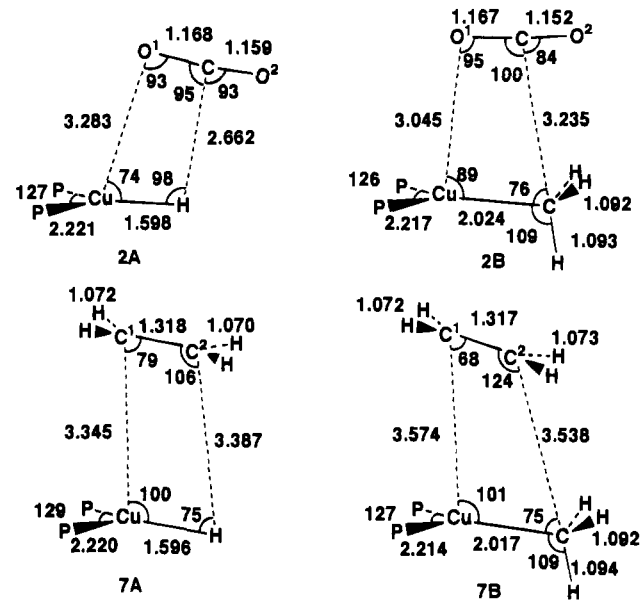

Figure 1. Optimized geometries of precursor complexes in the CO_2 and C_2H_4 insertions into the Cu–H and Cu–CH_3 bonds. Bond lengths are given in Å and angles in degree.

explained. The difference between =C=O and =C(O–)– bond energies is about 100 kcal/mol, about 30 kcal/mol greater than the difference between >C=C< and -CH_2-CH_2- bond energies. Thus, the E(=C(O–)–) – E(=C=O) term is not responsible for the higher exothermicity of the CO_2 insertion. The H_3C–CH_3 bond energy does not differ very much from the H_3C–C(O)OR bond energy (see Table 4), yielding only a little difference in the exothermicity between the CO_2 and C_2H_4 insertion reactions. On the other hand, E(Cu–OC(O)R) is larger than E(Cu–CH_3) by ca. 50 kcal/mol, indicating that the term, E(Cu–OC(O)R) – E(Cu–CH_3), is responsible for the greater exothermicity of the CO_2 insertion than that of the C_2H_4 insertion. In other words, the greater exothermicity of the CO_2 insertion is because the Cu–OC(O)CH_3 bond is stronger than the Cu–CH_3 bond.

Similarly, exothermicities of the CO_2 and C_2H_4 insertion reactions into the Cu–H bond are represented by eqs 11 and 12, respectively. The difference, E(=C=O) – E(=C(O–)–),

$$\begin{aligned} E_{exo} &= E(\text{Cu–OC(O)H}) + E(=\text{C(O–)–}) + \\ &\qquad E(\text{H–C(O)OR}) - E(\text{Cu–H}) - E(=\text{C=O}) \\ &= E(\text{Cu–OC(O)H}) + \{E(=\text{C(O–)–}) - \\ &\qquad E(=\text{C=O})\} + E(\text{H–C(O)OR}) - E(\text{Cu–H}) \quad (11) \end{aligned}$$

$$\begin{aligned} E_{exo} &= E(\text{Cu–C}_2\text{H}_5) + E(-\text{CH}_2\text{–CH}_2\text{–}) + \\ &\qquad E(\text{H–C}_2\text{H}_5) - E(\text{Cu–H}) - E(>\text{C=C}<) \\ &= E(\text{Cu–C}_2\text{H}_5) + \{E(-\text{CH}_2\text{–CH}_2\text{–}) - \\ &\qquad E(>\text{C=C}<)\} + E(\text{H–C}_2\text{H}_5) - E(\text{Cu–H}) \quad (12) \end{aligned}$$

is larger than the difference, E(>C=C<) – E(–CH_2–CH_2–), as discussed above. E(H–C(O)OR) is calculated to be similar to E(H–C_2H_5), as shown in Table 4. Thus, these two terms cannot explain the greater exothermicity of the CO_2 insertion into the Cu–H bond. On the other hand, E(Cu–OC(O)H) is much larger than E(Cu–C_2H_5). This is a major reason for the greater exothermicity of the CO_2 insertion into the Cu–H bond than that of the C_2H_4 insertion.

Precursor Complexes (PC), Transition States (TS), and the Activation Energies (E_a). Geometries of PC and TS are shown in Figures 1 and 2, respectively. In the PCs, the Cu–

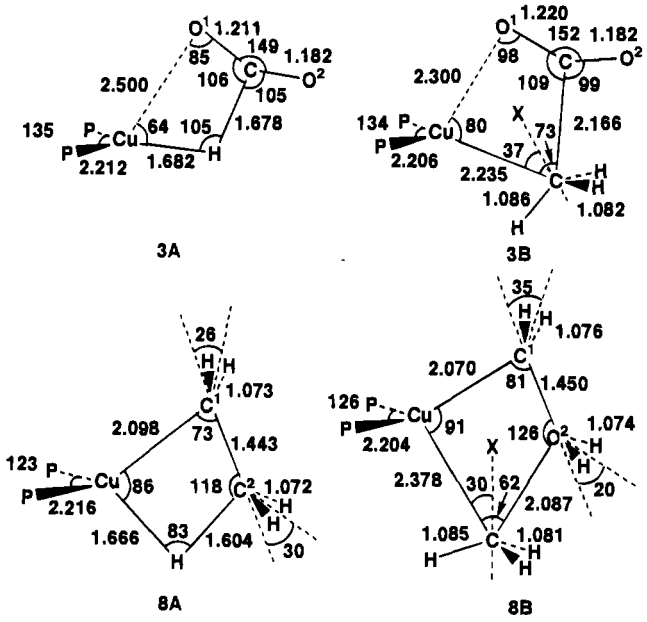

Figure 2. Optimized geometries of transition state in the CO_2 and C_2H_4 insertions into the Cu−H and Cu−CH_3 bonds. Bond lengths are given in Å and angles in degree.

Chart 1

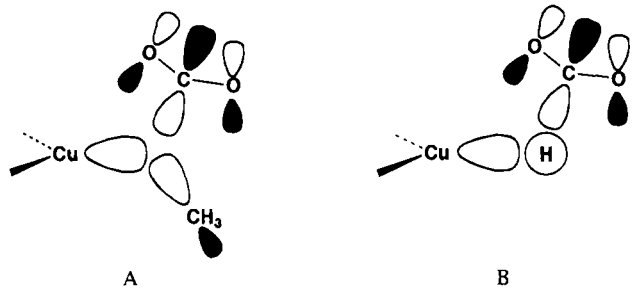

CO_2 and Cu−C_2H_4 distances are considerably longer than and the geometries of CO_2, C_2H_4, and $CuR(PH_3)_2$ parts only slightly distorted from those of the reactants. Consistent with these geometrical features, stabilization energies of PCs (Tables 2 and 3) are much smaller than that of the usual coordinate bond, indicating that CO_2 and C_2H_4 weakly interact with $CuR(PH_3)_2$ like a van der Waals complex.

In the TS of the CO_2 insertion into the Cu−H bond (**3A** in Figure 2), both C−H and Cu−O^1 distances between CO_2 and $CuH(PH_3)_2$ are much longer than those in the product. The Cu−H and C−O^1 bonds lengthen somewhat by ca. 0.1 Å and ca. 0.05 Å respectively, and the CO_2 part starts to bend (<OCO = 150°). Similar features are observed in the TS of the CO_2 insertion into the Cu−CH_3 bond (**3B** in Figure 2). There is, however, a critical difference between **3A** and **3B**; the CH_3 ligand moves considerably downward and changes its direction toward the incoming CO_2 molecule, whereas the H ligand only moves slightly downward at the TS. This difference between $CuH(PH_3)_2$ and $Cu(CH_3)(PH_3)_2$ is easily interpreted in terms of the valence orbitals of CH_3 and H ligands. Because of the highly directional sp^3 valence orbital, the CH_3 ligand must change its direction toward CO_2 in order to form a new bond with CO_2. At the same time, the CH_3 ligand wants to keep a bonding interaction with Cu as much as possible. Thus, the downward movement of CH_3 occurs to satisfy these two requisites, as schematically shown in Chart 1A. On the other hand, the H ligand does not need to change its position because it can form a new bond with the incoming CO_2, keeping the coordinate bond with Cu, due to its spherical 1s valence orbital (Chart 1B).

Chart 2

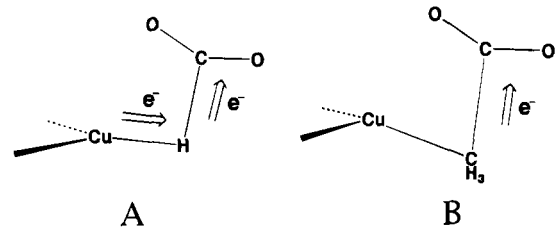

The TS of the C_2H_4 insertion into the Cu−R bond (R = H or CH_3) exhibits interesting features (Figure 2), as follows: (1) the Cu−H distance slightly lengthens but the Cu−CH_3 bond lengthens considerably, (2) both H and CH_3 ligands move considerably downward, (3) the C^1−C^2 bond of C_2H_4 lengthens considerably by 0.13 Å, and the C^1H_2 and C^2H_2 planes are remarkably bent back by 26 and 30°, respectively, and (4) the Cu−C^1 distance is short (2.1 Å) like that in the product, but the C^2−R bond is still long. These features suggest that the TS of the C_2H_4 insertion is product-like compared to the TS of the CO_2 insertion and that the Cu−C^1 bond is formed prior to the formation of the C^2−R bond (remember that both Cu−O^1 and C−R bonds between CO_2 and $CuR(PH_3)_2$ are not yet formed at the TS of the CO_2 insertion). These differences between CO_2 and C_2H_4 insertion reactions will be discussed below.

Activation energies (E_a) of these insertion reactions are given in Tables 2 and 3. Both CO_2 and C_2H_4 insertion reactions into the Cu−H bond occur with lower activation energies than those into the Cu−CH_3 bond. This result can be interpreted in terms of the valence orbitals of H and CH_3 ligands, again; as described above, the $CuH(PH_3)_2$ part distorts at the TS to a lesser extent than the $Cu(CH_3)(PH_3)_2$ part because the 1s valence orbital of H is spherical but the sp^3 valence orbital of CH_3 is directional. Accordingly, the insertion into the Cu−CH_3 bond needs a higher activation energy, due to the greater distortion energy of the $Cu(CH_3)(PH_3)_2$ part. Consistent with this result, Darensbourg et al. experimentally suggested that CO_2 could insert into the Ni−H bond but not into the Ni−CH_3 bond.[27m] The other interesting result to be noted is that the C_2H_4 insertion requires a higher activation energy than the CO_2 insertion, which will be discussed after investigating characters of the TS.

Electron Redistribution in the CO_2 and C_2H_4 Insertion Reactions and the Reason for Rather Low Activation Energy of the CO_2 Insertion. Changes in Mulliken populations by these reactions are shown in Figure 3. In all the insertion reactions examined, electron populations of CO_2 and C_2H_4 remarkably increase as the reaction proceeds, indicating that the charge-transfer from $CuR(PH_3)_2$ to CO_2 or C_2H_4 takes place during these reactions. In the insertion into the Cu−H bond, electron populations of both Cu and H significantly decrease (Figure 3A,C). This implies that the insertion into the Cu−H bond causes the charge-transfer from the H ligand to CO_2 or C_2H_4 concomitantly with the polarization of $CuH(PH_3)_2$ which induces electron flow from Cu to H (Chart 2A). In the insertion into the Cu−CH_3 bond, on the other hand, only the electron population of CH_3 decreases considerably, but the electron population of Cu hardly changes (Figure 3B,D), indicating that insertion into the Cu−CH_3 bond causes only charge-transfer to CO_2 or C_2H_4 from the CH_3 ligand (Chart 2B), unlike insertion into the Cu−H bond. This difference between R = CH_3 and R = H is easily interpreted in terms of the directionality of the valence orbital, again. Because the Cu−CH_3 bond must be broken to form a new CH_3−CO_2 bond at the TS due to the

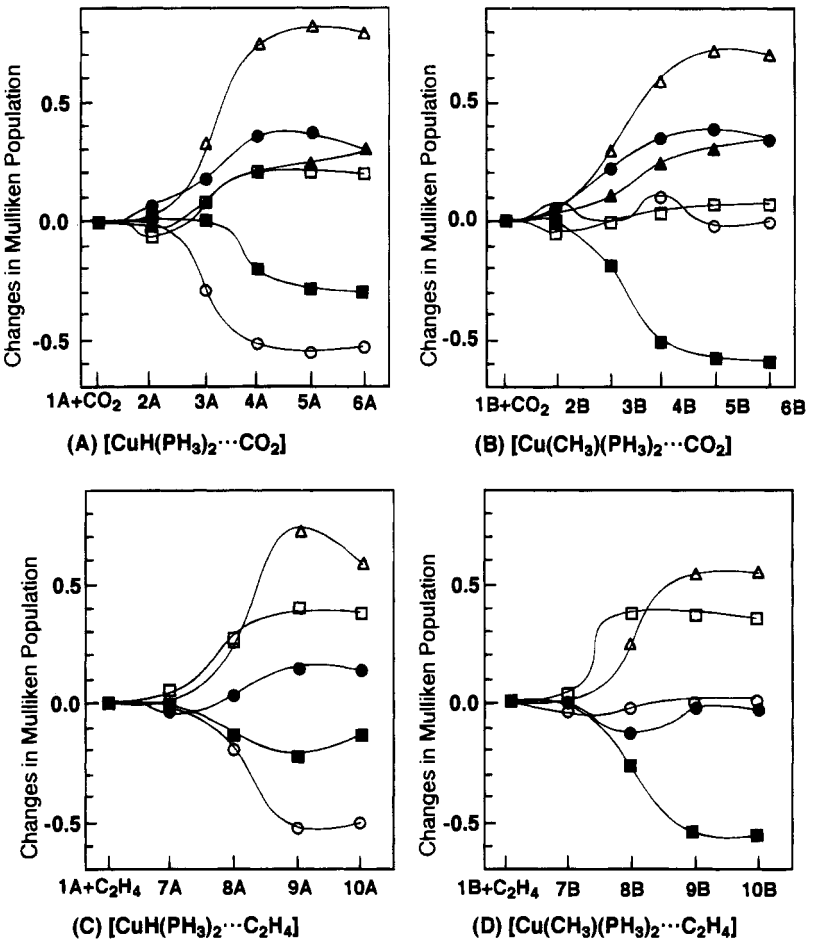

Figure 3. Changes in Mulliken populations caused by CO_2 and C_2H_4 insertions into the Cu−H and Cu−CH_3 bonds: (A) CO_2 insertion into the Cu−H bond; (B) CO_2 insertion into the Cu−CH_3 bond; (C) C_2H_4 insertion into the Cu−H bond; (D) C_2H_4 insertion into the Cu−CH_3 bond.

Scheme 2

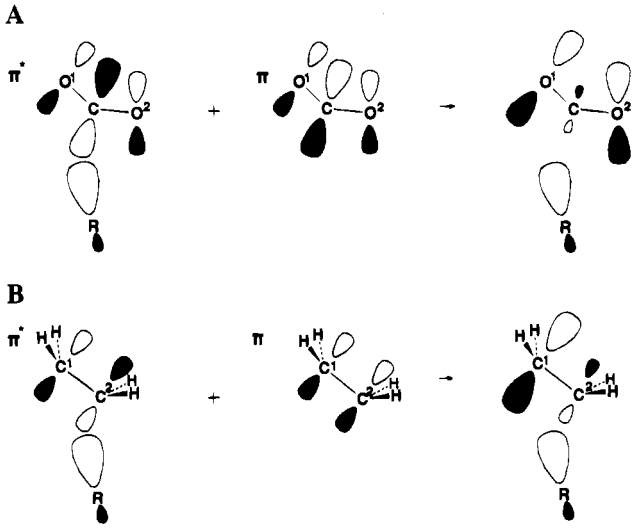

directional sp^3 valence orbital of CH_3, the electron flow from Cu to CH_3 becomes difficult around the TS. On the other hand, the electron flow from Cu to H can occur, because the Cu−H bond still exists at the TS due to the spherical 1s valence orbital of H.

Electron redistribution at the TS can be investigated in more detail by inspecting the difference density maps (Figure 4): $\varrho[CuR(PH_3)_2\cdot\cdot Sub]_{TS} - \varrho[CuR(PH_3)_2] - \varrho[Sub]$, where Sub means CO_2 or C_2H_4. An important feature found in the CO_2 insertion (Figure 4A) is that electron density accumulates on the terminal O atoms but slightly decreases on the central C atom (a similar feature is observed in the CO_2 insertion into the Cu−CH_3 bond, the picture of which is omitted here for brevity). This feature arises from the HOMO, $\Psi_{HOMO}(CuR\cdot\cdot CO_2)$, of the reaction system. This $\Psi_{HOMO}(CuR\cdot\cdot CO_2)$ resembles quite well the HOMO, $\Psi_{HOMO}(CO_2\cdot\cdot R^-)$, of the $CO_2\cdot\cdot R^-$ system, as clearly shown in Figure 4C,E. Both $\Psi_{HOMO}(CuR\cdot\cdot CO_2)$ and $\Psi_{HOMO}(CO_2\cdot\cdot R^-)$ mainly consist of the large p_π orbital of O, the very small p_π orbital of C, and the HOMO of R^-, which are formed through orbital mixing among the π and π^* orbitals of CO_2 and the HOMO of R^-; as shown in Scheme 2A, the HOMO of R^- overlaps with the π^* orbital of CO_2 in a bonding manner, into which the π orbital of CO_2 mixes in an antiboding manner with the HOMO of R^- because the former lies at lower energy than the latter. This orbital mixing decreases the p_π orbital of C but enhances the p_π orbital of O, which leads to accumulation of electron density on the O atoms but a slight decrease of electron density on the C atom, as we have seen in Figure 4A.

In the C_2H_4 insertion, electron density accumulates on the C^1 atom but decreases on the C^2 atom (see Figure 4B, a similar feature is observed in the C_2H_4 insertion into the Cu−CH_3 bond, the picture of which is omitted here to save the pages). This feature is explained in terms of the HOMO of the reaction system, $\Psi_{HOMO}(CuR\cdot\cdot C_2H_4)$, again. As shown in Figure 4D,F, this HOMO resembles quite well the HOMO of the $C_2H_4\cdot\cdot R^-$ system, $\Psi_{HOMO}(C_2H_4\cdot\cdot R^-)$. The HOMO, which mainly consists of the large p_π orbital of C^1, the small p_π orbital of C^2,

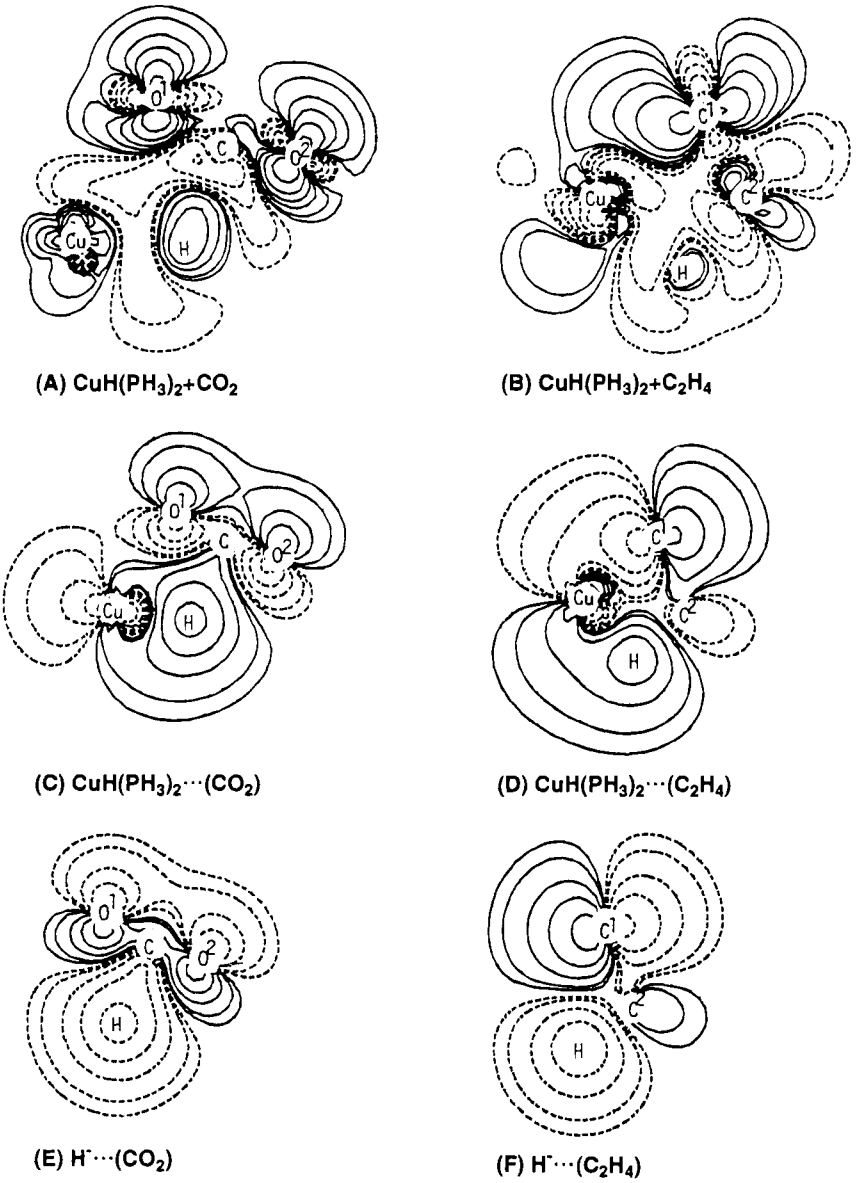

Figure 4. Maps of difference density (A and B) and HOMO at the transition state of CO_2 and C_2H_4 insertions into the Cu−H bond (C−F): (A) $[CuH(PH_3)_2\cdot\cdot\cdot(CO_2)]$, **3A**; (B) $[CuH(PH_3)_2\cdot\cdot\cdot(C_2H_4)]$, **9A**; (C) $[CuH(PH_3)_2\cdot\cdot\cdot(CO_2)]$; **3A**, (D) $[CuH(PH_3)_2\cdot\cdot\cdot(C_2H_4)]$, **9A**; (E) $CO_2\cdot\cdot\cdot H^-$; (F) $C_2H_4\cdot\cdot\cdot H^-$. Key: (a) countour values for density are ±0.05, ±0.02, ±0.01, ±0.005, ±0.002, and ±0.01; (b) contour values for contour are ±0.2, ±0.1, ±0.05, ±0.02, and ±0.01.

and the HOMO of R^-, are formed through the orbital mixing among the π and π^* orbitals of C_2H_4 and the HOMO of R^-; the HOMO of R^- overlaps with the π^* orbital of C_2H_4 in a bonding manner, into which the π orbital of C_2H_4 mixes in an antibonding manner with the HOMO of R^- because the former lies at lower energy than the latter, as shown in Scheme 2B. This orbital mixing enhances the C^1 p_π orbital but decreases the C^2 p_π orbital in $\Psi_{HOMO}(C_2H_4\cdot\cdot\cdot R^-)$ and $\Psi_{HOMO}(CuR\cdot\cdot\cdot C_2H_4)$, which leads to an increase of electron density on the C^1 atom but a decrease of electron density on the C^2 atom.

Electron redistribution in the region between R and Sub (Sub = CO_2 or C_2H_4) is important for the insertion reaction. At the TS of the CO_2 insertion, electron density accumulates in this region (Figure 4A). Actually, the considerable C−R bonding overlap between CO_2 and $CuR(PH_3)_2$ is observed in the Ψ_{HOMO}-$(CuR\cdot\cdot\cdot CO_2)$ (Figure 4C). At the TS of the C_2H_4 insertion, on the other hand, electron density decreases in this region (Figure 4B). Because the $\Psi_{HOMO}(CuR\cdot\cdot\cdot C_2H_4)$ involves the considerable C^2−R bonding overlap between C_2H_4 and $CuR(PH_3)_2$, like that in the CO_2 insertion (Figure 4D), the decrease in the density arises not from the $\Psi_{HOMO}(CuR\cdot\cdot\cdot C_2H_4)$ but from the other interaction, i.e., exchange repulsion between the π orbital of C_2H_4 and the HOMO of R. Approach of C_2H_4 to R would be difficult due to this strong exchange repulsion, which disfavors the C_2H_4 insertion into the Cu−R bond and leads to the high activation energy. In the case of the CO_2 insertion, this kind of exchange repulsion would be small because the π orbital of CO_2 lies considerably lower in energy (−19.37 eV) than that of C_2H_4 (−9.63 eV).[51] Accordingly, the C_2H_4 insertion requires a higher activation energy than the CO_2 insertion.

Finally, an interaction between Cu and Sub will be investigated. At the TS of the CO_2 insertion, electron density decreases in the region between Cu and O^1 atoms (Figure 4A). At the TS of the C_2H_4 insertion, on the other hand, electron density increases in this region (Figure 4B). Consistent with this result, $\Psi_{HOMO}(CuR\cdot\cdot\cdot C_2H_4)$ at the TS of the C_2H_4 insertion involves a strong bonding interaction between Cu and C^1 atoms (Figure

(51) Geometries of CO_2 and C_2H_4 were taken to be the same as the distorted structures like in the TSs of their insertion reactions into the Cu−H bond.

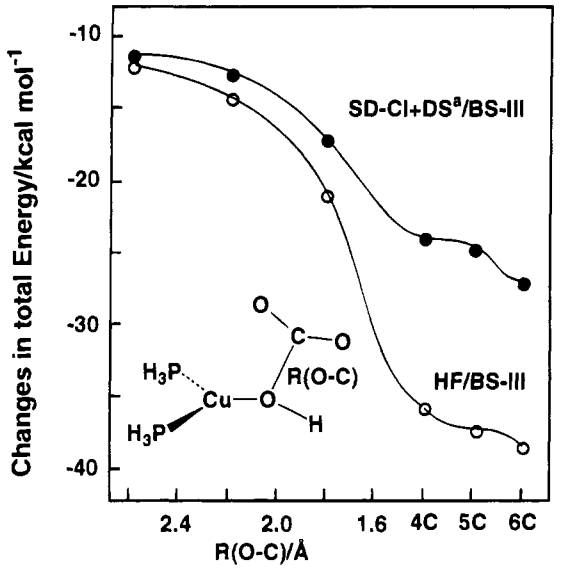

Figure 5. Changes in total energy caused by the CO_2 insertion into the Cu−OH bond of $Cu(OH)(PH_3)_2$, **1C**.

4D), while $\Psi_{HOMO}(CuR\cdots CO_2)$ at the TS of the CO_2 insertion involves an apparently weaker bonding interaction between Cu and O^1 atoms than that between Cu and C^1 atoms in Ψ_{HOMO}-$(CuR\cdots C_2H_4)$ (Figure 4C). All these features are consistent with the TS structure in which the Cu−C^1 distance is short at the TS of the C_2H_4 insertion but the Cu−O^1 distance is long at the TS of the CO_2 insertion. The short Cu−C^1 and the long Cu−O^1 distances are explained in terms of HOMOs, $\Psi_{HOMO}(C_2H_4\cdots R^-)$ and $\Psi_{HOMO}(CO_2\cdots R^-)$. These HOMOs (Figures 4E and 4F) are calculated to be −2.61 eV for $CO_2\cdots H^-$, −2.52 eV for $CO_2\cdots CH_3^-$, 0.56 eV for $C_2H_4\cdots H^-$, and 0.07 eV for $C_2H_4\cdots CH_3^-$, where geometries are taken to be the same as those in the TSs. This means that approach of R^- to C_2H_4 yields the HOMO at considerably high energy but approach of R^- to CO_2 yields the HOMO at rather low energy. Accordingly, $\Psi_{HOMO}(C_2H_4\cdots R^-)$ can form a much stronger charge transfer interaction with Cu than does $\Psi_{HOMO}(CO_2\cdots R^-)$, leading to the short Cu−C^1 distance at the TS of the C_2H_4 insertion. The Cu−O^1 distance is, however, rather long at the TS because the charge transfer from $\Psi_{HOMO}(CO_2\cdots R^-)$ to Cu is not very strong.

CO_2 Insertion Reaction into the Cu−OH Bond of Cu-$(OH)(PH_3)_2$. Interestingly, the CO_2 insertion into the Cu−OH bond proceeds with no barrier, as clearly shown in Figure 5. The following geometry changes are observed (Figure 6): the Cu−OH distance is getting longer, the Cu−O^1 distance is getting shorter, and the $\angle O^1CO^2$ angle gradually closes. All these results indicate that the Cu−OH bond is gradually broken, the Cu−O^1 bond is gradually formed, and the Cu−OC(O)OH bond is smoothly produced. The geometry at the late stage of this reaction is very close to that of the product, $Cu(\eta^1\text{-}OCO(OH))$-$(PH_3)_2$ (**4C**) (see the geometry at $R(O-CO_2)$ = 1.6 Å). After the insertion, **4C** converts to **5C** with a very small barrier (ca. 2.6 kcal/mol at the MP2/BS III level) and **5C** converts to the final product, $Cu(\eta^2\text{-}O_2COH)(PH_3)_2$ (**6C**), with no barrier (Figure 5).

Energy change by this insertion reaction considerably depends on electron correlation. Calculations at both HF and SD−CI levels, however, show that this insertion proceeds with no barrier. Unexpectedly, the exothermicity of this insertion (27.1 kcal/mol for **6C** (SD−CI(P)/BS III)) is calculated to be much smaller than that of the CO_2 insertion into Cu−H and Cu−CH_3 bonds, whereas CO_2 can insert into the Cu−OH with no barrier. The exothermicity of this insertion is approximately represented by eq 13.[50] The HO−C(O)OH bond energy is

$$E_{exo} = E(Cu-OC(O)OH) + E(HO-C(O)OH) + E(=C(O-)-) - E(Cu-OH) - E(=C=O)$$

$$E_{exo} = \{E(Cu-OC(O)OH) - E(Cu-OH)\} + \{E(=C(O-)-) - E(=C=O)\} + E(HO-C(O)OH) \quad (13)$$

estimated to be 87 kcal/mol, only slightly smaller than the C−C(O)OH bond energy (92 kcal/mol) (Table 4). On the other hand, the term E(Cu−OC(O)OH) − E(Cu−OH) is calculated to be 29 kcal/mol, much smaller than the term E(Cu−OC(O)R) − E(Cu−R), as shown in Table 4. Consequently, this insertion is less exothermic than the CO_2 insertion into the Cu−H and Cu−CH_3 bonds.

No activation energy of this insertion can be interpreted in terms of the HOMO of $Cu(OH)(PH_3)_2$ **1C**. Unlike the HOMOs of **1A** and **1B**, the HOMO of **1C** mainly consists of a lone-pair type orbital of OH^- which is not used for a coordinate bond with Cu (structure **I**). As a result, the LUMO of CO_2 can easily

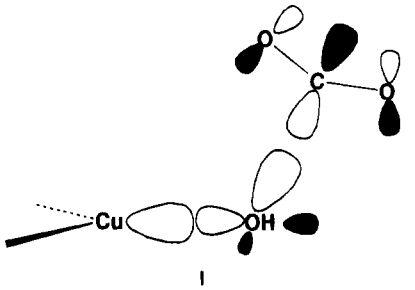

I

interact with this orbital. This means that the bonding interaction between CO_2 and OH is formed without weakening the Cu−OH bond. On the other hand, both H and CH_3 ligands have only one valence orbital which is used for bonding with Cu in **1A** and **1B**. Accordingly, the CO_2 insertion into the Cu−H bond weakens the Cu−H bond even though the 1s valence orbital of H is spherical, and the CO_2 insertion into the Cu−CH_3 bond considerably weakens the Cu−CH_3 bond because of the directional sp^3 valence orbital of CH_3. Thus, the CO_2 insertion into the Cu−OH bond occurs more easily than the CO_2 insertion into the Cu−H and Cu−CH_3 bonds.

Concluding Remarks

Ab initio MO/MP4, SD−CI, and CCD calculations are carried out on the insertion reactions of CO_2 and C_2H_4 into the Cu−R bond (R = H, CH_3, and OH). The activation energy (E_a) is calculated to be very low (ca. 4−5 kcal/mol) for the CO_2 insertion, relatively high (9−10 kcal/mol) for the C_2H_4 insertion into the Cu−H bond, and very high (23−30 kcal/mol) for the C_2H_4 insertion into the Cu−CH_3 bond. These results suggest that the C_2H_4 insertion into the Cu−R bond is more difficult than the CO_2 insertion into the Cu−R bond. The difference of E_a between CO_2 and C_2H_4 insertion reactions can be interpreted in terms of the exchange repulsion between R and Sub (Sub = CO_2 or C_2H_4); because the π orbital of C_2H_4 lies higher in energy than that of CO_2, the exchange repulsion between C_2H_4 and R is much larger than that between CO_2 and R, leading to the higher E_a value of the C_2H_4 insertion. The exothermicity of the CO_2 insertion is much greater than that of the C_2H_4 insertion. The main reason for the greater exothermicity of the CO_2 insertion is that E(Cu−OC(O)H) is larger than E(Cu−C_2H_5) and E(Cu−CH_3) by ca. 50 kcal/mol. CO_2 insertion into the Cu−OH bond proceeds with no barrier. This is because

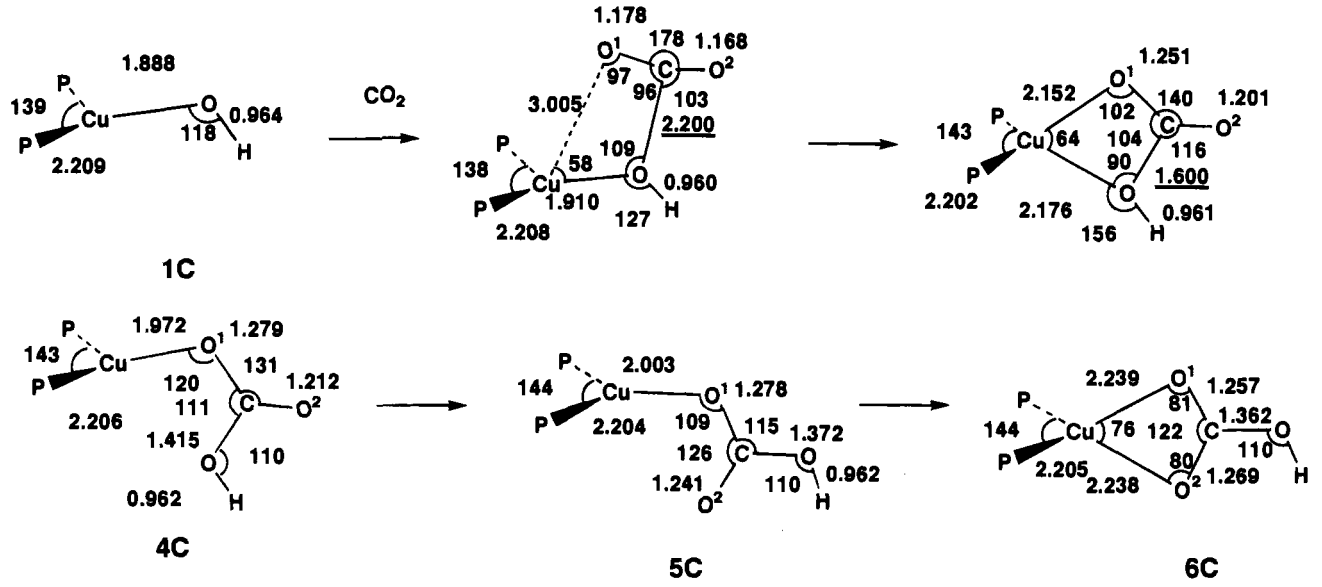

Figure 6. Changes in geometry caused by the CO_2 insertion into the Cu−OH bond of $Cu(OH)(PH_3)_2$, **1C**. Bond distances are given in Å and bond angles in degree.

the HOMO of $Cu(OH)(PH_3)_2$ mainly consists of the lone-pair type orbitals of OH^-, and the bonding interaction between CO_2 and OH can be formed without weakening of the Cu−OH bond. However, E_{exo} of this insertion is smaller than that of the other CO_2 insertion, since the Cu−OC(O)OH bond energy is about 29 kcal/mol larger than the Cu−OH bond energy (remember that the Cu−OC(O)R bond energy is about 50 kcal/mol larger than the $Cu-CH_3$ bond energy).

From these results, one can predict a primarily important factor for the CO_2 insertion is the presence of a lone-pair type orbital of R which is not used for coordination to Cu. When the R ligand possesses such a lone-pair type orbital, the bonding interaction between this lone-pair type orbital and the LUMO of CO_2 can be formed without weakening of the Cu−R bond. This situation facilitates the CO_2 insertion into the Cu−OH bond.

Acknowledgment. A Hitachi S-820 computer of the Institute for Molecular Science (Okazaki, Japan) and an IBM-340 work station of our laboratory were used for these calculations. This work is partially supported by a Grant-in-Aid from the Ministry of Education, Culture, and Science (Japan) (Nos. 04243102 and 06227256).

IC931341Z